Tetrahedron 73 (2017) 3079–3085

Contents lists available at ScienceDirect

Tetrahedron

journal homepage: www.elsevier.com/locate/tet

Design and synthesis of a second-generation ligand-tethered calcium indicator for plant cell biology based on the fundamental analyses of the structure and physical property

Yousuke Takaoka [a, b], Masaki Imai [a], Miyuki Shigenaga [a], Minoru Ueda [a, *]

[a] Department of Chemistry, Graduate School of Science, Tohoku University, 6-3 Aramaki-Aza-Aoba, Aoba-ku, Sendai 980-8578, Japan
[b] Precursory Research for Embryonic Science and Technology PREST, Japan, Science and Technology Agency, JST, 4-1-8 Honcho, Kawaguchi, Saitama 332-0012, Japan

ARTICLE INFO

Article history:
Received 9 March 2017
Received in revised form
5 April 2017
Accepted 11 April 2017
Available online 12 April 2017

Keywords:
Calcium probe
Plant cell
Chemical biology

ABSTRACT

Calcium ion (Ca^{2+}) is one of the most important second messengers. However, conventional Ca^{2+} indicators cannot be applied in plant cells. In previous paper, we developed the first-generation protein-ligand tethered calcium indicator that can be applied for living plant cells.

Here, we will report the development of second-generation indicator based on the detailed examination on physical properties of the first-generation to improve the drawbacks. Through the examination, we also found that cell permeability of the probe is strongly affected by their aggregation properties. Our findings will provide new strategy for the design of synthetic indicators.

1. Introduction

In plant cell biology, calcium ion (Ca^{2+}) is one of the most important second messengers. This ion is involved in the responses to numerous physiological stimuli, such as osmotic stress, cold shock, and stomatal closure triggered by drought stress.[1–6] However, conventional synthetic Ca^{2+} indicators cannot be applied in plant cells, mainly due to the presence of the cell wall and vacuole.[7–9] The cell wall prevents the penetration of most probes into cells, and small molecule that do penetrate the cell wall accumulate in the vacuole. Thus, small molecular Ca^{2+} indicators cannot provide information on the cytosolic Ca^{2+} concentration in plant cells. Control of intracellular localization is indispensable for the development of Ca^{2+} indicators for living plant cells. Recently, we developed a protein ligand-tethered Ca^{2+} indicator[10] composed of an analogue of a natural product-based protein ligand, synthetic ligand of FKBP12 (SLF),[11–14] and a fluorescent Ca^{2+} indicator, Calcium Green-1 (CaGreen-1)[15–17] (Fig. 1, **1a** – **c**). Proof of principle experiments using tobacco (*Nicotiana tabacum*) BY-2 cells over-expressing human FKBP12 demonstrated that one of our functionalized indicator **1b** showed efficient cell permeability and localized within the cytosol and nucleus due to the SLF ligand that bound specifically to FKBP12. Therefore, this indicator enabled spatiotemporal monitoring of Ca^{2+} ions in living BY-2 cells.

Despite these advances, the development of Ca^{2+} indicators for plant cells is still in its infancy. Reliable strategies to improve cell permeability and sensitivity under changing Ca^{2+} concentrations are needed. Firstly, the sensitivity of these indicators is very low. They showed as little as two-fold increases in fluorescence intensity between the presence and absence of Ca^{2+} ions. To improve the Ca^{2+} sensitivity of the probe, it is important to discover why the **1**-series shows such a low level of fluorescence enhancements compared with that of the intact fluorophore. Secondly, the differences in cell permeability among probes **1a** – **1c** could not be explained only by structural differences. Only probe **1b** could penetrate into cells and provide strong fluorescence, whereas probes **1a** and **1c** could not penetrate cells at all. Fundamental analyses are required to explain why only probe **1b** shows cell permeability.

In this study, we improved the synthetic route of probes **1a** – **1c** so that they can reliably supplied for further research. Analyses of their physical properties strongly suggested that their aggregation properties affect their permeability into BY-2 cells. We also designed and synthesized SLF-conjugated Fluo-4 derivatives (**2a**, **b**) as second-generation highly sensitive Ca^{2+} indicators. Overall, our results will lead to new insights into the molecular design of

* Corresponding author.
E-mail address: ueda@m.tohoku.ac.jp (M. Ueda).

http://dx.doi.org/10.1016/j.tet.2017.04.023
0040-4020/

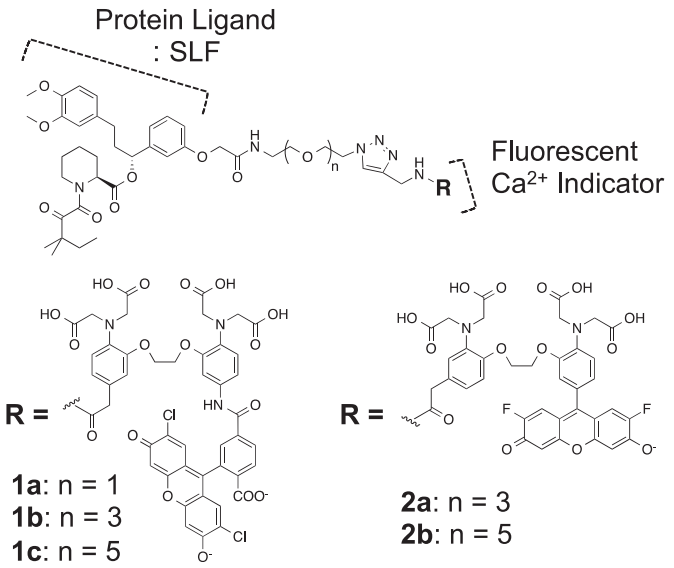

Fig. 1. Chemical structures of SLF-tethered calcium indicators used in this study.

fluorescent indicators that can be practically applied in research on plant cells.

2. Results and discussion

2.1. Improvement of synthetic scheme of alkyne-tethered CaGreen-1

A synthetic supply of SLF-tethered CaGreen-1 (**1a** – **1c**) was strongly desirable for further research on the factors affecting cell permeability. However, our previous syntheses (Scheme S1) resulted in very low yields, such as a total yield of 0.6% for **3**.[10] The low synthetic yield could be largely attributed to two troublesome steps: the reduction of the nitro group (compound **3**–**3** and **3**–**6**, yields of 66% and 41%, respectively); and alkylation to construct the *O,O′*-Bis(2-aminophenyl)ethyleneglycol- *N,N,N′,N′*-tetraacetamide (BAPTA) moiety (compound **3**–**4**, crude yield of approx. 35%). In addition, the resulting probe **3** was obtained as a mixture of 5- and 6-isomers on the carboxydichlorofluorescein moiety because the amount of **3** obtained was too small for further purification.

We improved the synthetic route as shown in Scheme 1 to supply appropriate amounts of **1a** – **1c** for detailed analyses. 5-Hydroxy-4-nitrophenylacetic acid was protected as the *tert*-butyl ester, and coupled with **3**–**1** to provide **4**–**2**. Catalytic hydrogenation using Pd/C provided the corresponding diamine **4**–**3** quantitatively. The resulting **4**–**3** was smoothly alkylated to provide **4**–**4** with a 79% yield. This improved alkylation yield was because **4**–**3** was more soluble than the previous intermediate **3**–**3**. Then, the total yield of **4**–**8** was improved to approx. 13% which corresponds to 20-fold the yield of the corresponding reaction from **3**–**7** in our previous route. The ample supply of **4**–**8** enabled the purification of the 5- and 6-isomers (**4**–**9** and **4**–**10**) by HPLC to give 5- and 6-isomers of alkyne-tagged CaGreen-1 (**4a** and **4b)** after hydrolysis. Each isomer was coupled with azide-tagged SLF (**5a** – **5c**) via a copper (I)-catalyzed alkyne-azide cycloaddition (CuAAC) reaction to give the SLF-tethered CaGreen-1 (**1a** – **1c**) as per the previous procedure. The resulting pure isomers of SLF-tethered CaGreen-1 were subjected to further analyses.

2.2. Conjugation position between chromophore and BAPTA does not affect fluorescence enhancement

We have already reported that our SLF-tethered CaGreen-1 (**1b**) showed as little as two-fold fluorescence enhancement upon addition of Ca^{2+}. The enhancement ratio was much lower than that of the original CaGreen-1, which showed as much as five-fold fluorescence enhancement under these experimental conditions. A similar small fluorescence enhancement (two-fold) was observed for alkyne-tethered CaGreen-1 (**3**) as a mixture of 5- and 6- isomers. Therefore, we concluded that these decreases in the fluorescence response were possibly due to the derivatization of the CaGreen-1 fluorophore. In general, the fluorescence enhancement of such fluorescein-based Ca^{2+} indicators upon addition of Ca^{2+} ions is dependent on the efficiency of photo-induced electron transfer (PeT) between the aniline group of BAPTA and the fluorophore in Ca^{2+}-free conditions. Therefore, the efficiency of PeT in **3** might be severely decreased compared with that in the original CaGreen-1 because the installed alkyl group would affect the intramolecular configuration of the CaGreen fluorophore and the BAPTA moiety. Thus, we supposed that the positions of the installed alkyl group, the 5- or 6-position, may affect the efficiency of PeT in **3**.

We compared the fluorescence response of the two purified isomers, **4a** as the 6-isomer and **4b** as the 5-isomer, to determine whether the position of alkylation between carboxydichlorofluorescein and BAPTA affected fluorescence. As shown in Fig. S1, **4a** and **4b** showed almost the same saturation curve upon addition of Ca^{2+}, and their fluorescence enhancements were about 2.0 and 2.1-fold, respectively. These values were comparable to those reported previously for 5-,6-mixtures **(3** in Scheme S1). In the previous reports by Martin et al., Fluo-4 derivatives in which dextran or biotin was installed in the BAPTA moiety showed almost half the fluorescence enhancement compared with that of the original Fluo-4 (fluorescence enhancement of dextran- or biotin-conjugated Fluo-4 was 70-fold or 105-fold, respectively, and that of the original one was 200-fold).[17] This result roughly correlated with our results for **4a** and **4b**. Note that the fluorescence spectra of **3** or **4a/b** in the absence of Ca^{2+} were relatively higher than that of the original CaGreen-1, whereas those after addition of high concentrations of Ca^{2+} were almost the same (Fig. S1). Therefore, it can be concluded that the two conjugation positions (6- and 5-) equally affected the efficiency of PeT in **4a** and **4b**, and increased the background fluorescence in the absence of Ca^{2+} leading to the decrease in the fluorescence enhancement upon addition of Ca^{2+}. CaGreen-1 has a relatively high quantum yield even without Ca^{2+}. In addition, the introduction of the BAPTA moiety to the CaGreen-1 fluorophore further decreased the fluorescence response as mentioned above. Thus, we concluded that the low Ca^{2+}-sensitivity could be attributed to the molecular design of the Ca^{2+}-indicator. Consequently, a new molecular design, such as replacement of the fluorophore, was necessary to improve sensitivity.

2.3. Physical properties affecting cell permeability of CaGreen-1 derivatives

It was difficult to determine the reason for the distinct differences in cell permeability among **1a** – **1c** because the only difference among them was the number of ethylene glycol units in the linker moiety. Such a small change in polarity should not affect cell permeability. However, several recent reports have suggested that the “aggregation properties” of amphiphilic molecules in aqueous media are strongly affected by the structure of the linker between hydrophobic and hydrophilic groups.[18–21] In our study, the probes consisted of a hydrophobic SLF ligand and a relatively hydrophilic Ca^{2+} indicator. Thus, we initially focused on the aggregation properties of **1a** – **1c** in aqueous media.

Dynamic light scattering (DLS) measurements of **1a** or **1c** in buffer solution consistently showed aggregates with a mean

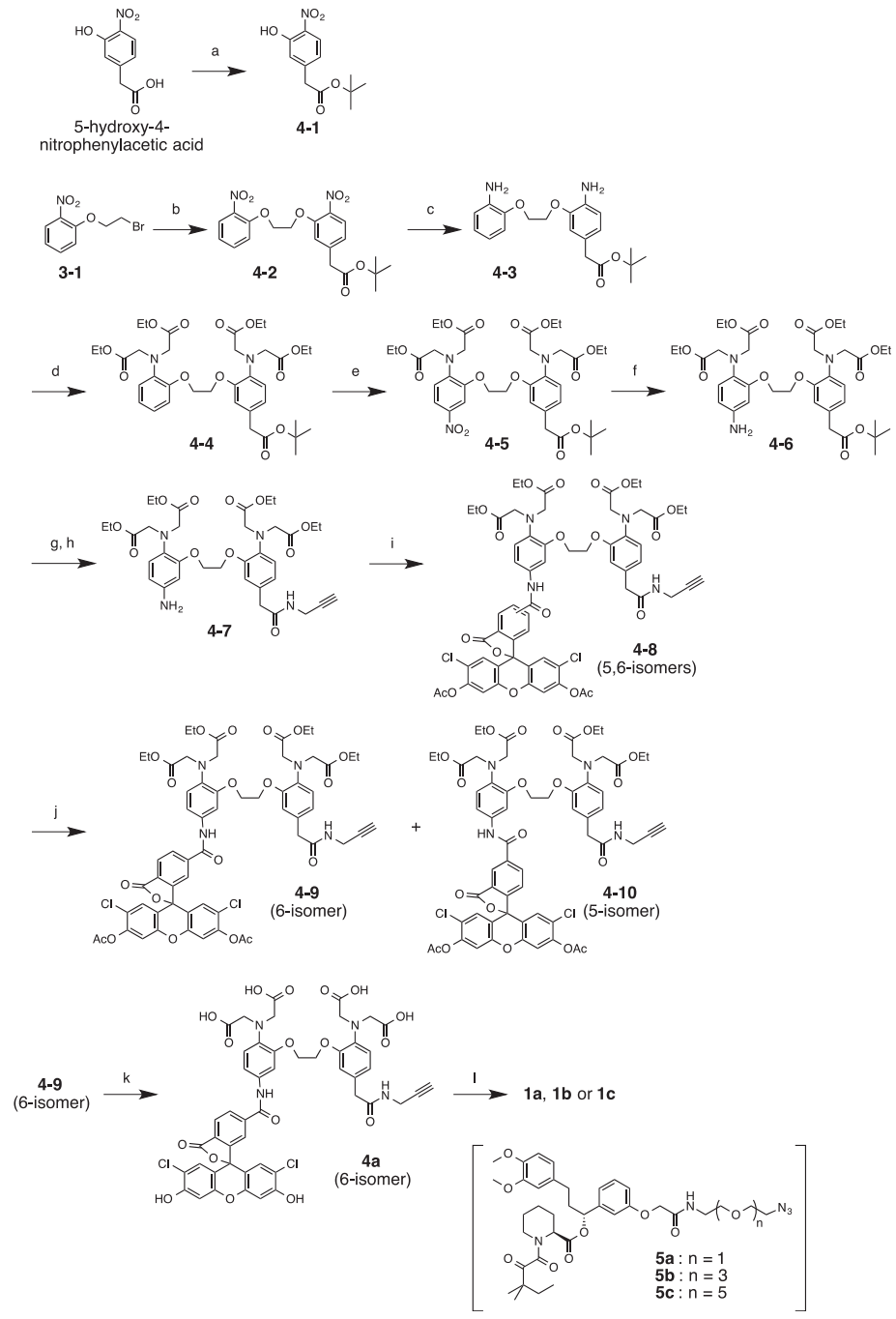

Scheme 1. Synthetic scheme of compound **4a**. *Reaction conditions:* a) *t*-BuOH, water soluble carbodiimide hydrochloride (WSC·HCl), 4-dimethylaminopyridine (DMAP) in dry dimethylformamide (DMF), 71%; b) *N,N*-diisopropylethylamine (DIPEA) in dry DMF, 79%; c) Pd/C, H_2, quant.; d) ethyl bromoacetate, DIPEA in dry CH_3CN, 79%; e) HNO_3, $NaNO_2$ in AcOH, f) Pd/C, H_2 in MeOH, 53% (2 steps); g) trifluoroacetic acid (TFA) in CH_2Cl_2, h) propargylamine, WSC·HCl, HOBt·H_2O, DIPEA in dry DMF, 67% (2 steps); i) 5(6)-carboxy-2′,7′-dichlorofluorescein diacetate, HATU, DIPEA in dry DMF, j) HPLC purification, k) KOH aq., MeOH, quant. l) **5a** – **5c**, CuI, sodium ascorbate, DIPEA, DMF.

diameter of approximately 100 nm (Fig. 2a). In contrast, **1b** showed almost no scattering at the same concentration (2 μM), and in the solution containing 10 μM probe, distinct scattering was observed. The critical aggregation concentration (CAC) values were 2, 10 and 5 μM for **1a**, **1b**, and **1c**, respectively (Fig. 2b). These results clearly indicated that the self-assembly properties and aggregate sizes of **1a** – **1c** drastically differed depending on the length of the linker. These aggregates were scarcely but definitely observed in a 100 nM solution of the probes in scattering intensity-based analyses (Fig. S3). The results indicated that the cell permeability of SLF-tethered CaGreen-1 was possibly due to the self-assembling property of the probe; that is, only probe **1b** showed efficient cell permeability, which had the highest CAC value and was least likely to self-assemble among our SLF-tethered CaGreen-1 probes. This result provides promising insights into the design of synthetic indicators that will remain effective in living plant cells. The aggregation property is tightly linked to the cell permeability of the synthetic probe, and can be fine-tuned by adjusting the structure and length of the linker moiety.

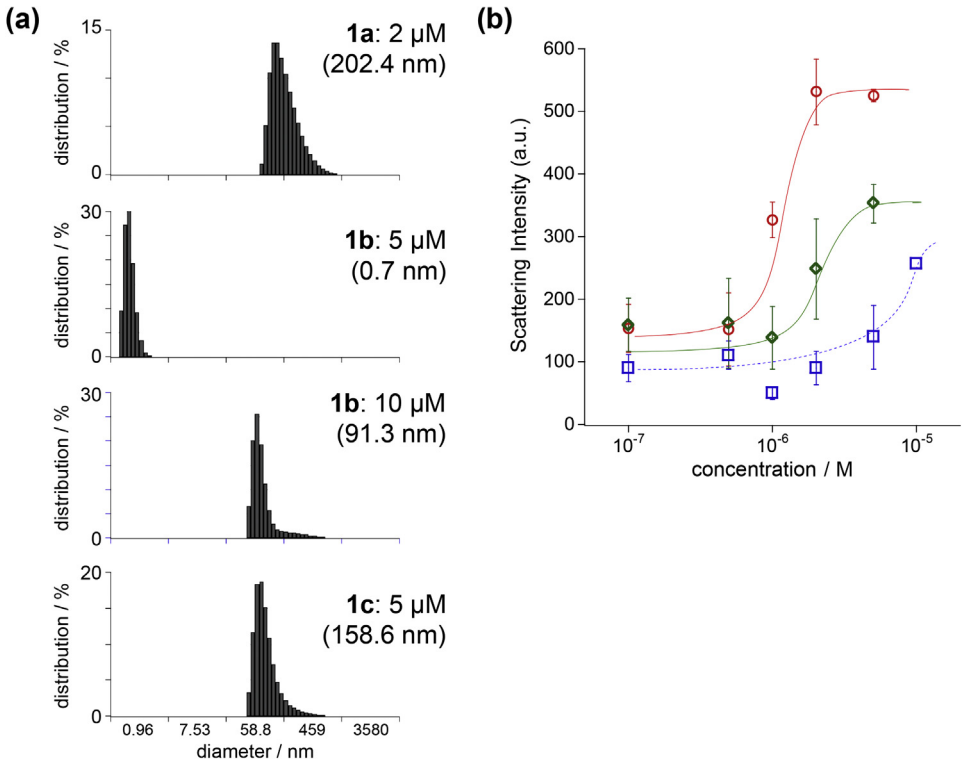

Fig. 2. (a) Dynamic light scattering (DLS) analyses of probes **1a** – **1c** in culture medium. (b) Concentration-dependent change of scattering intensities of probes **1a** (◯, red), **1b** (◇, green) and **1c** (, blue). Data were collected from DLS analyses with the same laser intensity and sensitivity. Experiments were performed in triplicate to obtain mean and s.d. values (shown as error bars).

2.4. Development of protein ligand-tethered Fluo-4 derivatives

Next, we designed a new Ca^{2+} indicator equipped with Fluo-4 instead of CaGreen-1 as the fluorophore to address the two disadvantages of first-generation Ca^{2+} indicator **1b**; that is, the low Ca^{2+}-sensitivity and the control of cell permeability. We prepared the alkyne-tagged Fluo-4 derivative **6**–**8** according to Scheme S2.[22] Then, **6**–**8** was connected to SLF-azide derivatives via the CuAAC reaction as reported previously. We prepared two probes (**2a** and **2b**) with an O3-type or O5-type linker structure between the SLF and Fluo-4 moieties. As shown in Fig. 3a and b, the fluorescence enhancement upon addition of Ca^{2+} was more than 25-fold for **2a** and 70-fold for **2b**. Also, the enhancements showed a typical saturation curve. The CAC value of **2a** was about 2 μM, the same as that of the non-cell-permeable probe **1a** (Fig. 3c). In contrast, the CAC value of **2b** with the O5-type linker was about 10 μM, comparable to that of our first-generation indicator **1b** with good cell permeability (Fig. 3c, d). In conclusion, we have successfully developed a second-generation SLF-tethered Ca^{2+} indicator, **2b**, which has improved Ca^{2+} sensitivity and is expected to have good cell permeability.

3. Conclusion

In this work, we improved the synthetic route to produce alkyne-tethered CaGreen-1 probes (**4a/b**) and examined their performance in detail. *In vitro* Ca^{2+} titration experiments revealed that the lower Ca^{2+} sensitivity of **4a/b** compared with that of the original CaGreen-1 could attributed to the structural modification of the BAPTA moiety. The marked differences in cell permeability among **1a** – **1c**, which were easily prepared from **4a/b**, were related to differences in their aggregation properties. It is very interesting that subtle differences in the linker length drastically affect the cell permeability of indicators. The scattering analyses of these indicators implied that a cell-permeable probe (having the O3-type linker, **1b**) was well solubilized in cultured medium, whereas non-cell permeable probes (**1a** or **1c**) formed self-assembling aggregates in the medium at a low concentration. This result provides a useful guideline for the molecular design of synthetic probes: that is, cell permeability is strongly affected by their aggregation properties, which can be fine-tuned by adjusting the structure and length of the linker moiety. Based on these results, we have designed and synthesized a second-generation Ca^{2+} indicator for the use in plant cells (**2b**). Compared with **1b**, **2b** has improved Ca^{2+} sensitivity and is expected to have good cell permeability. The application of the new probes to detect Ca^{2+} signaling in living plant cells is now in progress. Our findings may lead to the development of a new general strategy for the design of synthetic indicators for use in living plant cells and animal cells.

4. Experimental

4.1. General materials and methods

Both ^{1}H and ^{13}C NMR spectra were recorded on a JNM-ECS-400 (JEOL Inc., Japan) spectrometer in deuterium chloroform or deuterium methanol. High-resolution (HR) electrospray ionization (ESI)-mass spectrometry (MS) analyses were conducted using a microTOF II (Bruker Daltonics Inc., Germany) mass spectrometer with ESI techniques. Reagents and solvents were purchased from Kanto Chemical Co. Ltd., Japan; Wako Pure Chemical Industries Co. Ltd., Japan; and Nacalai Tesque Co., Ltd., Japan. All anhydrous solvents were dried using standard techniques and freshly distilled before use or purchased from Wako in their anhydrous form. All

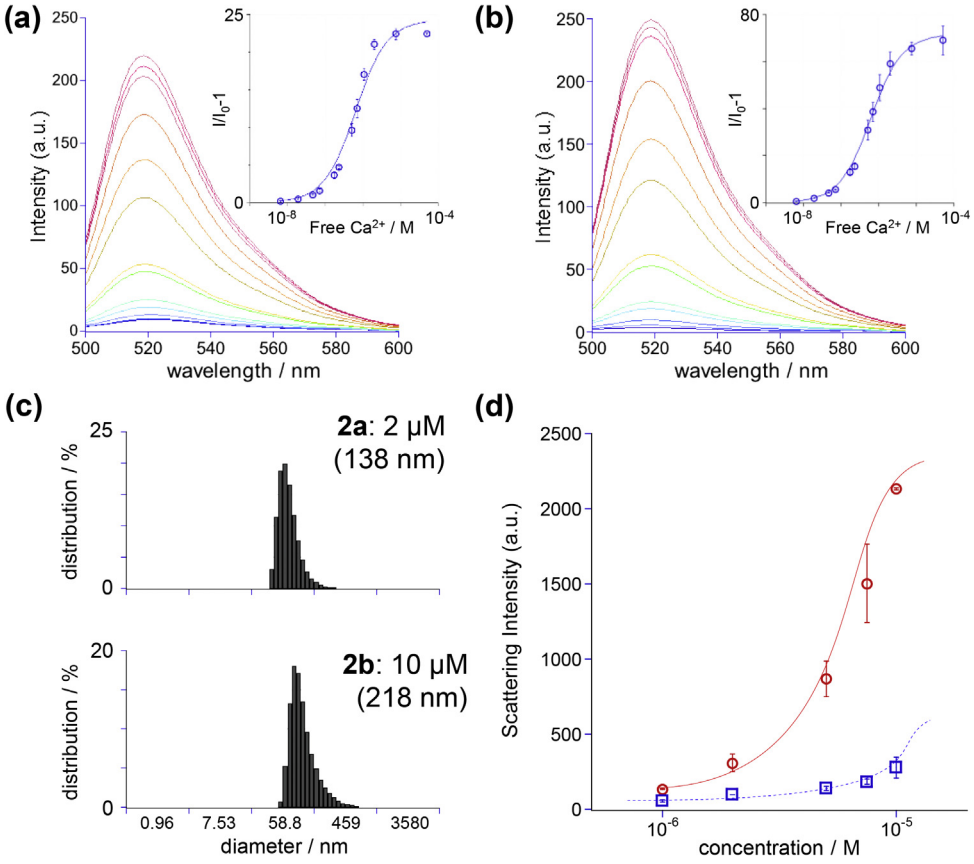

Fig. 3. (a, b) Fluorescence spectra of probe **2a** (a) or **2b** (b) (100 nM) upon addition of Ca^{2+} in buffer (inset; Ca^{2+} titration curve showing typical saturation). (c) Dynamic light scattering (DLS) analyses of probes **1a** – **1c** in culture medium. (d) Concentration-dependent change of scattering intensities of probes **2a** (○, red) and **2b** (, blue). Data were collected from DLS analyses with the same laser intensity and sensitivity. Experiments were performed in triplicate to obtain mean and s.d. values (shown as error bars).

flash chromatography was carried out using dry-packed Chromatorex PSQ 100B silica gel (Fuji Silysia Chemical Co., Ltd., Japan). Reactions were monitored by thin layer chromatography, carried out on Kieselgel 60 PF254 (Merck, Germany) 0.2 mm plates. Unless stated otherwise, all reactions were carried out under air. HPLC purifications were performed on a JASCO PU-2089 plus system (JASCO MD-2018). The DLS measurements were performed under the same conditions using various concentrations of probes on Zetasizer Nano ZS (Malvern Instruments) with a square-type cell. A DMSO stock solution of each compound was slowly added to the buffer solution to give a final concentration of 100 nM to 10 μM. All measurements were carried out in triplicate.

4.2. Calcium ion titration experiments in test tube

All probes were dissolved in DMSO to generate stock solutions. The concentrations of CaGreen-1 probes (**1a** – **1c**) were determined by their absorbance at 506 nm in 0.1N NaOH aq. using a molar extinction coefficient of 81,000 $M^{-1}cm^{-1}$.[23] The concentrations of Fluo-4 probes (**2a**, **2b**) were determined by their absorbance at 494 nm in 0.1N NaOH aq. using a molar extinction coefficient of 88,000 $M^{-1}cm^{-1}$.[23] All experiments were performed at 25 °C. Ultraviolet–visible absorption spectra were recorded on a Shimadzu UV–visible 2600 spectrometer. Fluorescence spectra were measured using a JASCO FP-6300 or FP-8500 fluorescence spectrometer. In the Ca^{2+} titration experiments, the probe concentration was 100 nM in 50 mM HEPES buffer (pH 7.4, 100 mM NaCl) containing *O,O′*-Bis(2-aminoethyl)ethyleneglycol-*N,N,N′,N′*-tetraacetic acid (EGTA) (final concentration, 1 mM) to captured the trace amounts of Ca^{2+}. During the Ca^{2+} titration using $CaCl_2$ aq. stock solution, the free Ca^{2+} concentration in 1 mM EGTA buffer was calculated with the MaxChelator program (Ca-EGTA Calculator v 1.2).[10]

4.3. Synthesis

4.3.1. Synthesis of 4–1

To a stirred solution of 5-hydoxy-4-nitrophenylacetic acid (653 mg, 3.31 mmol) and *tert*-butanol (7 mL) in dry DMF (14 mL) was added WSC·HCl (949 mg, 4.95 mmol, 1.5 eq) and DMAP (403 mg, 3.31 mmol, 1 eq). After the mixture was stirred at r.t. for 12 h, the solvent was evaporated. The residue was diluted with EtOAc and washed with 5% citric acid, distilled water and brine. The organic layer was dried over Na_2SO_4. The solvent was evaporated and the residue was purified by column chromatography (silica, $CHCl_3$:MeOH = 100:1) to afford **4**–**1** as a yellow oil (588 mg, 71%). ^1H NMR ($CDCl_3$, TMS, 400 MHz, r.t.): δ/ppm = 1.45 (s, 9H), 3.56 (s, 2H), 6.91 (dd, J = 1.6, 8.8 Hz, 1H), 7.07 (d, J = 1.6 Hz, 1H), 8.06 (d, J = 8.8 Hz, 1H), 10.60 (s, 1H). IR (film) 3240, 2980, 2935, 1732, 1626, 1589, 1482, 1445, 1369, 1329, 1274, 1256, 1144, 1085. HRMS (ESI, positive) m/z $[M+Na]^+$ calcd for $C_{12}H_{15}NO_5Na$ 276.0842, found 276.0847.

4.3.2. Synthesis of 4–2

To a stirred solution of **4**–**1** (588 mg, 2.32 mmol) and K_2CO_3 (641 mg, 4.64 mmol, 2 eq) in dry DMF (7.7 mL) was added **3**–**1**[24] (742 mg, 3.02 mmol, 1.3eq). The mixture was stirred at 105 °C for 4 h. The solvent was evaporated and the residue was diluted with

5% citric acid aq., and then extracted with EtOAc three times, and then the organic layer was washed with distilled water and brine. The organic layer was dried over Na_2SO_4. The solvent was evaporated and the residue was purified by column chromatography (silica, CH_2Cl_2:hexane = 1:1 to 2:1, and then 1:0) to afford **4**–**2** as a clear oil (764 mg, 79%). ^{1}H NMR ($CDCl_3$, TMS, 400 MHz, r.t.): δ/ppm = 1.46 (s, 9H), 3.62 (s, 2H), 4.54 (m, 4H), 6.98(dd, J = 1.6, 8.4, 1H), 7.06–7.10 (m, 1H), 7.16 (d, J = 2.0, 1H), 7.25 (dd, J = 1.2, 8.4, 1H), 7.55–7.59 (m, 1H), 7.81–7.84 (m, 2H). ^{13}C NMR ($CDCl_3$, 400 MHz, r.t.): δ/ppm = 28.0, 42.4, 68.6, 68.6, 81.7, 115.8, 116.8, 121.3, 122.2, 125.5, 125.7, 134.3, 138.8, 140.3, 142.0, 151.8, 152.0, 169.4. IR (film) 2979, 2933, 1729, 1607, 1523, 1352, 1254, 1280, 1145, 1092. HR-ESI-MS: Calcd. for $[M(C_{20}H_{22}N_2O_8)+Na]^+$: m/z = 441.1274; Found: 441.1287.

4.3.3. Synthesis of 4–3

To a stirred solution of **4**–**2** (500 mg, 1.20 mmol) in MeOH (2.5 mL) and CH_2Cl_2 (2.5 mL) was added Pd/C (100 mg). The mixture was stirred under H_2 at r.t for 3 h. After the reaction, the suspension was filtrated through celite. The solvent was evaporated to afford **4**–**3** as a white solid (479 mg, quant.). ^{1}H NMR ($CDCl_3$, TMS, 400 MHz, r.t.): δ/ppm = 1.43 (s, 9H), 3.41 (s, 2H), 3.78–3.83 (b, 2H), 4.37 (m, 4H), 6.66–6.74 (m, 4H), 6.79–6.87 (m, 3H).

4.3.4. Synthesis of 4-4

To a stirred solution of **4**–**3** (479 mg, 1.20 mmol) in dry CH_3CN (20 mL) was added DIPEA (2025 μL, 12.0 mmol, 10eq) and ethyl bromoacetate (1.06 mL, 9.6 mmol, 8eq). The mixture was stirred and refluxed for 5 h, and ethyl bromoacetate (1 mL, 9.6 mmol, total 16 eq) was added. The mixture was stirred and refluxed over night. After reaction, the solvent was evaporated. The residue was diluted with distilled water and extracted with EtOAc, and the combined organic layer was washed with brine. The organic layer was dried over Na_2SO_4. The solvent was evaporated and the residue was purified by column chromatography (silica, AcOEt:hexane = 1:3) to afford **4**–**4** as a yellow solid (663 mg, 79%). ^{1}H NMR ($CDCl_3$, TMS, 400 MHz, r.t.): δ/ppm = 1.12–1.16 (m, 12H), 1.43 (s, 9H), 3.42 (s, 2H), 3.00–4.07 (m, 8H), 4.13–4.15 (m, 8H), 4.27 (m, 4H), 6.73–6.92 (m, 7H). ^{13}C NMR ($CDCl_3$, 400 MHz, r.t.): δ/ppm = 13.9, 13.9, 28.0, 42.2, 53.4, 53.4, 60.7, 60.7, 66.9, 80.6, 113.0, 113.7, 118.7, 118.8, 121.4, 121.9, 122.0, 128.5, 138.0, 139.3, 150.1, 150.2, 170.8, 171.5. IR (film) 2981, 2933, 1747, 1508, 1369, 1246, 1178, 1027. HR-ESI-MS: calcd. for $[M(C_{36}H_{50}N_2O_{12})+Na]^+$: m/z = 725.3261; found: 725.3249.

4.3.5. Synthesis of 4–6

To a stirred solution of **4**–**4** (200 mg, 0.285 mmol) in AcOH (1 mL) was added 70% HNO_3 aq. (19 μL, 0.314 mmol, 1.1eq) and $NaNO_3$ (2.0 mg, 0.029 mmol, 0.1eq). After stirring for 30 min, the mixture was poured into distilled water, and extracted with EtOAc (three times), and combined organic layer was washed with water (three times) and brine (twice). The organic layer was dried over Na_2SO_4. Excess AcOH was removed via azeotrope in toluene, to yield the crude product **4**–**5** a yellow oil (220 mg) was isolated. This compound was used for the next step without any purification.

4–**5:** ^{1}H NMR ($CDCl_3$, TMS, 400 MHz, r.t.): δ/ppm = 1.12–1.16 (m, 12H), 1.43 (s, 9H), 3.42 (s, 2H), 4.02–4.09 (m, 8H), 4.13–4.15 (m, 8H), 4.28–4.32 (m, 4H), 6.68 (d, J = 9.2 Hz, 1H), 6.76 (m, 3H), 7.73 (d, J = 2.8 Hz, 1H), 7.84 (DMSO-$d_6$dd, J = 9.2, 2.8 Hz, 1H). IR (film) 3382, 2981, 2933, 1743, 1588, 1517, 1331, 1249, 1181, 1026. ESI-MS: calcd. for $[M+Na]^+$: m/z = 770.311; found: 770.284.

To a stirred solution of **4**–**5** (213 mg, 0.285 mmol) in MeOH (3 mL) and CH_2Cl_2 (2 mL) was added Pd/C (20 mg). The mixture was stirred under H_2 at r.t for 3 h. After reaction, the suspension was filtrated through celite. The solvent was evaporated and the residue was purified by column chromatography (silica, AcOEt:hexane = 1:2 to AcOEt:$CHCl_3$ = 1:1 (1% MeOH)) to afford **4**–**6** as a yellow amorphous compound (108 mg, 0.15 mmol, 53% (2steps)). ^{1}H NMR ($CDCl_3$, 400 MHz, r.t.): δ/ppm = 1.14–1.18 (m, 12H), 1.43 (s, 9H), 3.42 (s, 2H), 3.52 (b, 2H), 4.01–4.09 (m, 12H), 4.14 (s, 4H), 4.27 (m, 4H), 6.23 (dd, J = 2.4, 8.4, 1H), 6.31 (d, J = 2.4, 1H), 6.76–6.79 (m, 4H). ^{13}C NMR ($CDCl_3$, 400 MHz, r.t.): δ/ppm = 14.0, 28.0, 42.2, 53.5, 53.9, 60.5, 60.7, 67.1, 67.1, 80.7, 102.1, 107.7, 114.1, 119.0, 121.6, 122.0, 128.63, 131.42, 138.1, 142.5, 150.2, 152.0, 171.0, 171.6, 171.7.

4.3.6. Synthesis of 4–8

To a stirred solution of compound **4**–**6** (108 mg, 0.15 mmol) in CH_2Cl_2 (1 mL) was added TFA. The mixture was stirred at r.t. for 2 h. Excess TFA was removed via azeotrope with CH_3CN in toluene, yielding a crude product (178 mg). Then, to a stirred solution of the above crude product in dry DMF (2 mL) was added propargylamine (50 mg, 0.9 mmol, 6 eq), WSC·HCl (35 mg, 0.18 mmol, 1.2eq), HOBt·H_2O (27 mg, 0.18 mmol, 1.2eq), and DIPEA (78 μL, 0.45 mmol, 3eq). The mixture was stirred at r.t. for 16 h. The solvent was evaporated. The residue was diluted with EtOAc and washed with sat. $NaHCO_3$, distilled water and brine. The organic layer was dried over Na_2SO_4. The solvent was evaporated and the residue was purified by column chromatography (silica, $CHCl_3$:MeOH = 30:1) to afford compound **4**–**7** as a brown solid (62 mg, 59% in two steps) without any further purification. Finally, to a stirred solution of the above crude compound **4**–**7** in dry DMF (2 mL) was added 5(6)-carboxy-2,7-dichlorofluorescein (47 mg, 89 μmol, 1 eq), HATU (41 mg, 0.11 mmol, 1.2eq), and DIPEA (31 μL, 0.18 mmol, 2eq). The mixture was stirred at r.t. for 8 h. The solvent was evaporated. The residue was purified by column chromatography (silica, $CHCl_3$:MeOH = 30:1). The obtained solid was suspended in diisopropylether, filtered, and dried in vacuo to yield the 5,6-mixture of compound **4**–**8** (72 mg, 67%). The mixture of 5-, and 6-isomers of **4**–**8** was then purified by HPLC with a linear gradient (ODS, CH_3CN (0.05% TFA):H_2O (0.05% TFA) = 75:25 (5min) to 90:10 (55 min). By using the authentic samples of the 6- or 5-isomer of compound **4**–**8** prepared separately, the retention time of the 6-isomer was identified as 22 min and that of the 5-isomer was 18 min ^{1}H NMR of **4**–**9** (6-isomer) ($CDCl_3$:CD_3OD = 1:1, 400 MHz, r.t.): δ/ppm = 1.12–1.17 (m, 12H), 2.36–2.39 (m, 7H), 3.44 (s, 2H), 3.92–3.94 (m, 2H), 4.00–4.06 (m, 16H), 4.28 (m, 4H), 6.76–6.82 (m, 3H), 6.87 (m, 1H), 6.95 (s, 2H), 7.18 (d, J = 1.6 Hz, 1H), 7.28 (s, 2H), 7.32–7.39 (m, 2H), 7.81 (m, 1H), 8.20 (d, J = 8.0 Hz, 1H), 8.30 (dd, J = 1.2 Hz, 8.0 Hz, 1H). IR (film) 3299, 2927, 2850, 1776, 1733, 1672, 1605, 1516, 1411, 1371, 1259, 1200, 1167, 1026, 758. HRMS (ESI, positive) m/z $[M+H]^+$ calcd for $C_{60}H_{59}N_4O_{19}Cl_2$ 1209.3145, found 1209.3144.

4.3.7. Synthesis of 4a

To a stirred solution of compound **4**–**9** (6-isomer, 0.25 mg, 0.21 μmol) in MeOH (34 μL) was added 1N KOH aq. (21 μL). The mixture was stirred at r.t. for overnight. The solution was neutralized with 1N HCl aq. to pH 7, and lyophilized to afford **4a** (6-isomer) as a red solid (quant.) containing the inorganic salt. The amount of **4a** was calculated from the UV–vis absorption spectrum with the molar extinction coefficient of 2,7-dichlorofluorescein.[23]

Acknowledgement

We thank Prof. H. Isobe and Dr. S. Sota (Univ. of Tokyo) for the use of DLS. This work was supported in part by a Grant-in-Aid for Scientific Research (No. 26282207 to M.U. and No. 25708026, No. 16K13093 to Y.T.) on Innovative Areas “Chemical Biology of Natural Products” from MEXT, Japan, and by JST (No. JPMJPR16Q4 to Y.T.).

Appendix A. Supplementary data

Supplementary data related to this article can be found at http://dx.doi.org/10.1016/j.tet.2017.04.023.

References

1. Swanson SJ, Choi W-G, Chanoca A, Gilroy S. *Annu Rev Plant Biol*. 2011;62:273–297.
2. Lecourieux D, Ranjeva R, Pugin A. *New Phytol*. 2006;171:249–269.
3. Kiegle E, Moore CA, Haseloff J, Tester MA, Knight MR. *Plant J*. 2000;23:267–278.
4. Knight MR, Read ND, Campbell AK, Trewavas AJ. *J Cell Biol*. 1993;121:83–90.
5. Pel Z-M, Murata Y, Benning G, et al. *Nature*. 2000;406:731–734.
6. Allen GJ, Chu SP, Schumacher K, et al. *Science*. 2000;289:2338–2342.
7. Jones DL, Kochian LV, Gilroy S. *Plant Physiol*. 1998;116:81–89.
8. Bush DS, Jones RL. *Cell Calcium*. 1987;8:455–472.
9. Bush DS, Biswas AK, Jones RL. *Planta*. 1989;178:411–420.
10. Takaoka Y, Shigenaga M, Imai M, et al. *Bioorg Med Chem Lett*. 2016;26:9–14.
11. Tsukiji S, Miyagawa M, Takaoka Y, Tamura T, Hamachi I. *Nat Chem Biol*. 2009;5:341–343.
12. Komatsu T, Kukelyansky I, McCaffery JM, Ueno T, Varela LC, Inoue T. *Nat Methods*. 2010;7:206–208.
13. Ishida M, Watanabe H, Takigawa K, et al. *J Am Chem Soc*. 2013;135:12684–12689.
14. Keenan T, Yaeger DR, Courage NL, et al. *Bioorg Med Chem Lett*. 1998;6:1309–1335.
15. Tour O, Adams SR, Kerr RA, et al. *Nat Chem Biol*. 2007;3:423–431.
16. Bannwarth M, Corrêa Jr IR, Sztretye M, et al. *ACS Chem Biol*. 2009;4:179–190.
17. Martin VV, Beierlein M, Morgan JL, Rothe A, Gee KR. *Cell Calcium*. 2004;36:509–514.
18. Takaoka Y, Kiminami K, Mizusawa K, et al. *J Am Chem Soc*. 2011;133:11725–11731.
19. Yoshii T, Mizusawa K, Takaoka Y, Hamachi I. *J Am Chem Soc*. 2014;136:16635–16642.
20. Yagai S, Kitamura Y. *Chem Soc Rev*. 2008;37:1520–1529.
21. Lim YB, Moon KS, Lee M. *Chem Soc Rev*. 2009;38:925–934.
22. Gee KR, Brown KA, Chen WN, Bishop-Stewart J, Gray D, Johnson I. *Cell Calcium*. 2000;27:97–106.
23. Haugland RP. *The Handbook: A Guide to Fluorescent Probes and Labeling Technologies*. tenth ed. Carsbad, CA: Invitrogen; 2005.
24. Grynkiewicz G, Poenie M, Tsien RY. *J Biol Chem*. 1985;260:3440–3450.